Synthesis, Structure, and Reactivity of Alkylzinc Complexes Stabilized with 1,1,3,3-Tetramethylguanidine

Scott D. Bunge,* Jacob M. Lance, and Jeffrey A. Bertke

Department of Chemistry, Kent State University, Kent, Ohio 44242-0001

Received May 21, 2007

The synthesis and structural characterization of several novel alkylzinc guanidinate, alkoxide, and aryloxide complexes are reported. 1,1,3,3-Tetramethylguanidine, H-TMG, was successfully reacted with $(Et)_2Zn$ in a 4:3 and a 1:1 ratio to yield the corresponding linear $[Zn_3(\mu\text{-TMG})_4(Et)_2]$ (**1**) and cyclic $[Zn(\mu\text{-TMG})(Et)]_3$ (**2**) complexes. Further investigations have shown **2** to react with alcohols, HOR, to form complexes with the general formula $[Zn(Et)(OR)(H\text{-TMG})]_n$, where OR = $OCH_2C(CH_3)_3$ {ONep, $n = 2$ (**3**)}, $OC_6H_3(CMe_3)_2$-2,6 {DBP, $n = 1$ (**4**)}, and $OC_6H_2Bu^t_2$-2,6-Me-4 {DBP-4-Me, $n = 1$ (**5**)}. The addition of $(Et)_2Zn$ to a solution of **4** yielded the unusual $[Zn_2(\mu\text{-TMG})(\mu\text{-DBP})(Et)_2]$ (**6**). Complex **5** readily reacts with the alcohol, HOR′, yielding dinuclear compounds with the formula $[Zn(\mu\text{-OR}')(DBP\text{-4-Me})(H\text{-TMG})]_2$, where OR′ = OCH_3 (OMe, **7**) and OCH_2CH_3 (OEt, **8**). Additionally, compound **4** was reacted with EtOH, yielding a complex with the formula $[Zn(\mu\text{-OEt})(DBP)(H\text{-TMG})]_2$ (**9**). The utility of compound **8** for use as a catalyst in the ring-opening polymerization of *rac*-lactide was additionally investigated. Compounds **1**−**9** were characterized by single-crystal X-ray diffraction. The bulk powders for all complexes were found to be in agreement with the crystal structures based on elemental analyses, FT-IR spectroscopy, and ^1H and ^{13}C NMR studies. The polymer was characterized by multi-nuclear NMR spectroscopy and MALDI-TOF mass spectrometry.

Introduction

Alkylzinc (RZn) reagents have found extensive use in catalysis, organic synthesis, and also in materials science. Designing a co-ligand for RZn complexes to facilitate discrete stoichiometric and catalytic reactivity has traditionally involved a delicate interplay between the steric and electronic components of the auxiliary ligand and the coordinative saturation of the metal center.[1−3] A general strategy to achieving this balance would be the use of a conveniently obtained "versatile" ligand, capable of facilitating coordinative saturation while hindering entropically driven disassociation. One potential ligand possibly capable of achieving this interplay is the imine of tetramethylurea, the "super base" 1,1,3,3-tetramethylguanidine (H-TMG).

For the past 20 years, the use of H-TMG has been sporadic in the field of inorganic chemistry.[4] This deficiency is surprising because H-TMG belongs to one of the strongest and most versatile classes of organic bases known.[5] For comparison, they are several orders of magnitude more basic than tertiary amines.[6] Also, in addition to the strength, this enhanced basicity can be "tuned" due to the excellent distribution of charge over the resonance-stabilized guanidine structure.[7] In this Article, we present our effort to outline the stoichiometric reactivity of TMG-ligated and H-TMG-ligated ethylzinc systems with alcohols of varied steric bulk. Historically, in the absence of additional Lewis bases, Zn alkoxides and aryloxides have been found to form ill-defined polymetallic species.[8] The ability of H-TMG to support the isolation of well-defined systems is therefore also assessed in this study.

The synthesis of **1**−**9** was accomplished through examining derivations of one of the oldest known class of organometallic reactions: ethane elimination via reaction of diethyl zinc with various ratios of guanidine and alcohol.[9] The reaction of 4 and 3 equiv of H-TMG with 3 equiv of diethyl zinc, $(Et)_2Zn$, was performed. Products isolated from each reaction were found to be the novel trinuclear $[Zn_3(\mu\text{-TMG})_4(Et)_2]$ (**1**) and $[EtZn(\mu\text{-TMG})]_3$ (**2**), respectively (Scheme 1). The general reactivity of **2** was further investigated. **2** reacts with HOR to form complexes with the general formula $[Zn(Et)(OR)(H\text{-TMG})]_n$, where OR

* To whom correspondence should be addressed. Phone: (330) 672-9445. Fax: (330) 672-3816. E-mail: sbunge@kent.edu.

(1) Parkin, G. *Chem. Rev.* **2004**, *104*, 699. Cheng, M.; Moore, D. R.; Reczek, J. J.; Chamberlain, B. M.; Lobkovsky, E. B.; Coates, G. W. *J. Am. Chem. Soc.* **2001**, *123*, 8738. Darensbourg, D. J.; Holtcamp, M. W.; Struck, G. E.; Zimmer, M. S.; Niezgoda, S. A.; Rainey, P.; Robertson, J. B.; Draper, J. D.; Reibenspies, J. H. *J. Am. Chem. Soc.* **1999**, *121*, 107.

(2) Chisholm, M. H.; Gallucci, J.; Phomphrai, K. *Inorg. Chem.* **2002**, *41*, 2785.

(3) Jensen, T. R.; Breyfogle, L. E.; Hillmyer, M. A.; Tolman, W. B. *Chem. Commun.* **2004**, 2504.

(4) Kuhn, N.; Fawzi, R.; Steimann, M.; Wiethoff, J. *Z. Anorg. Allg. Chem.* **1997**, *623*, 554. Schneider, W.; Bauer, A.; Schier, A.; Schmidbaur, H. *Chem. Ber.* **1997**, *130*, 1417. De Vries, N.; Costello, C. E.; Jones, A. G.; Davison, A. *Inorg. Chem.* **1990**, *29*, 1348. Pattison, I.; Wade, K.; Wyatt, B. K. *J. Chem. Soc. A* **1968**, 837. Bailey, P. J.; Pace, S. *Coord. Chem. Rev.* **2001**, *214*, 91. Edwards, A. J.; Paver, M. A.; Raithby, P. R.; Rennie, M. A.; Russell, C. A.; Wright, D. S. *J. Chem. Soc., Dalton Trans.* **1995**, 1587. Stalke, D.; Paver, M. A.; Wright, D. S. *Angew. Chem., Int. Ed. Engl.* **1993**, *32*, 428. Davies, M. K.; Raithby, P. R.; Rennie, M. A.; Steiner, A.; Wright, D. S. *J. Chem. Soc., Dalton Trans.* **1995**, 2707. Alvarez, C. S.; Boss, S. R.; Burley, J. C.; Humphry, S. M.; Layfield, R. A.; Kowenicki, R. A.; McPartlin, M.; Rawson, J. M.; Wheatley, A. E. H.; Wood, P. T.; Wright, D. S. *Dalton Trans.* **2004**, 3481.

(5) Smith, P. A. S. *The Organic Chemistry of Open-Chain Nitrogen Compounds, Vol. I*; Benjamin: New York, 1965. Patai, S., Ed. *The Chemistry of Functional Groups: the Chemistry of Amidines and Imidates*; Wiley: Chichester, 1975.

(6) Kovacevic, B.; Maksic, Z. B. *Org. Lett.* **2001**, *3*, 1523. Kovacevic, B.; Maksic, Z. B. *Chem.-Eur. J.* **2002**, *8*, 1694. Novak, I.; Wei, X.; Chin, W. S. *J. Phys. Chem. A* **2001**, *105*, 1783.

(7) Coles, M. P. *Dalton Trans.* **2006**, 985.

(8) Caulton, K. G.; Hubertpfalzgraf, L. G. *Chem. Rev.* **1990**, *90*, 969.

(9) Menard, D. F.; Aston, J. G. *J. Am. Chem. Soc.* **1934**, *56*, 1601. Gilman, H.; Brown, G. E.; Webb, F. J.; Spatz, S. M. *J. Am. Chem. Soc.* **1940**, *62*, 977. Seyferth, D. *Organometallics* **2001**, *20*, 2940.

10.1021/om700501g CCC: $37.00
Publication on Web 11/07/2007

Scheme 1. Synthesis of 1 and 2

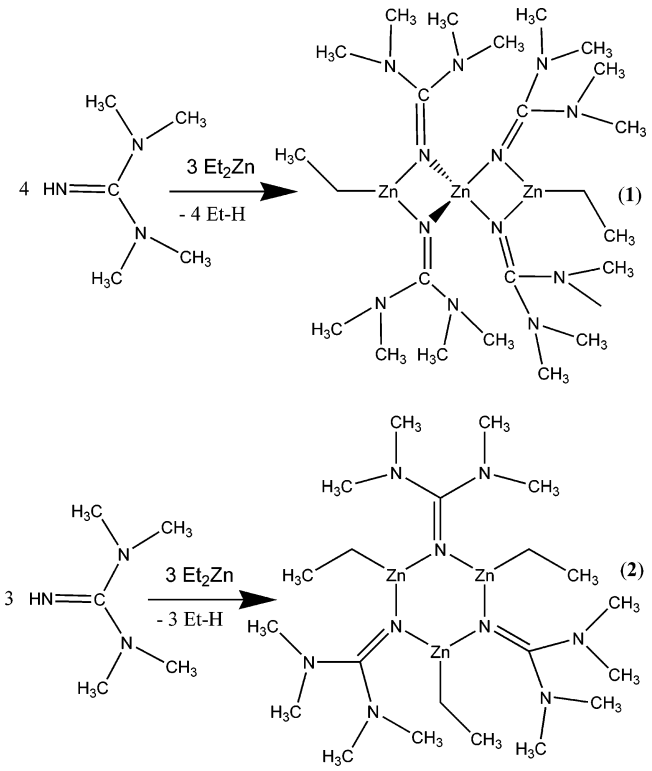

$= OCH_2C(CH_3)_3$ {ONep, $n = 2$ (**3**)}, $OC_6H_3(CMe_3)_2$-2,6 {DBP, $n = 1$ (**4**)}, and $OC_6H_2Bu^t_2$-2,6-Me-4 {DBP-4-Me, $n = 1$ (**5**)}. The addition of $(Et)_2Zn$ to a solution of **4** yielded $[Zn_2(\mu\text{-TMG})(\mu\text{-DBP})(Et)_2]$ (**6**). **5** readily reacts with HOR′, yielding dinuclear compounds: $[Zn(\mu\text{-OR}')(DBP\text{-4-Me})(H\text{-TMG})]_2$, where OR′ = OCH_3 (OMe, **7**) and OCH_2CH_3 (OEt, **8**). Furthermore, **4** was reacted with EtOH, yielding a complex with the formula $[Zn(\mu\text{-OEt})(DBP)(H\text{-TMG})]_2$ (**9**). The structures of these complexes are shown in Figures 1−7, respectively. In addition, a preliminary investigation utilizing **8** as a catalyst in the ring-opening polymerization of *rac*-lactide is also reported.

Experimental Section

All compounds were handled with rigorous exclusion of air and water using standard glovebox techniques. All anhydrous solvents were stored under argon and used as received in sure-seal bottles. $(Et)_2Zn$ (1.0 M in hexanes), H-TMG, H-ONEP, H-DBP, MeOH, EtOH, and *rac*-lactide were used as received from commercial suppliers. FT-IR data were obtained on a Bruker Tensor 27 Instrument using KBr pellets under an atmosphere of flowing nitrogen. Melting points were determined on samples sealed in a glass tube under an atmosphere of argon using an Electrothermal Mel-Temp apparatus and are uncorrected. Elemental analysis was performed on a Perkin-Elmer 2400 Series 2 CHN-S/O Elemental Analyzer.

Synthesis of 1 and 2. 1 and **2** were synthesized by adding the appropriate amount of $(Et)_2Zn$ (1.0 M) dropwise to a solution of H-TMG dissolved in hexanes (10 mL). After being stirred for 30 min, the reaction mixture was allowed to sit in the glovebox until the solvent evaporated and crystals formed. The complexes were subsequently recrystallized from a concentrated hexanes solution at −37 °C to obtain satisfactory elemental analysis.

$[Zn_3(\mu\text{-TMG})_4(Et)_2]$ (1). H-TMG (0.96 g, 8.3 mmol) and $(Et)_2Zn$ (4.4 g, 6.3 mmol) were used. Yield 97% (1.4 g, 2.0 mmol). Mp (dec) 140 °C. Anal. Calcd for $C_{24}H_{58}N_{12}Zn_3$: C, 40.54; H, 8.22; N, 23.64. Found: C, 40.41; H, 8.21; N, 23.91. ^{1}H NMR (400 MHz, toluene-d_8): δ = 2.71 (s, 48.0H, N=C(N(CH_3)$_2$)$_2$), 1.64 (t, 6.0H, CH_2CH_3), 0.62 (q, 4.0H, CH_2CH_3). ^{13}C{^{1}H} NMR (100.5 MHz, toluene-d_8): δ = 163.8 (N=*C*(N(CH_3)$_2$)$_2$), 39.9 (N=C(N(*C*H_3)$_2$)), 14.0 (CH_2CH_3), 4.5 (CH_2CH_3). FT-IR (KBr, cm^{-1}): 3058 (m), 2953 (s), 1546 (s), 1500 (m), 1457 (m), 1411 (s), 1372 (m), 1246 (s), 1196 (m), 1132 (s), 1101 (m), 1062 (m), 1033 (m), 987 (w), 959 (w), 920 (w), 901 (w), 880 (s), 859 (m), 816 (m), 787 (s), 754 (s), 662 (m) 622 (m), 569 (m), 530 (m), 467 (w), 443 (w).

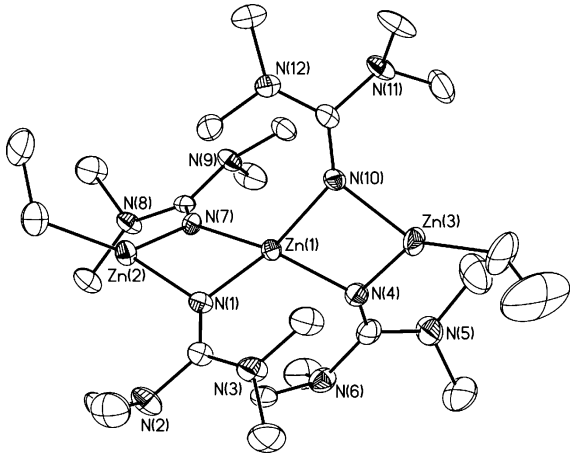

Figure 1. Thermal ellipsoid plot of **1**. Ellipsoids are drawn at the 30% level. H atoms have been omitted for clarity.

$[Zn(\mu\text{-TMG})(Et)]_3$ (2). H-TMG (0.72 g, 6.3 mmol) and $(Et)_2Zn$ (4.4 g, 6.3 mmol) were used. Yield 85% (1.1 g, 1.79 mmol). Mp 98 °C. Anal. Calcd for $C_{21}H_{51}N_9Zn_3$: C, 40.30; H, 8.21; N, 20.14. Found: C, 39.97; H, 8.11; N, 20.75. ^{1}H NMR (400 MHz, toluene-d_8): δ = 2.69 (s, 36.0H, 4N=C(N(*C*H_3)$_2$)$_2$), 1.54 (t, 9.0H, CH_2CH_3), 0.47 (q, 6.0H, CH_2CH_3). ^{13}C NMR (100.5 MHz, toluene-d_8): δ = 160.9 (N=*C*(N(CH_3)$_2$)), 40.4 (N=C(N(*C*H_3)$_2$)), 14.1 (CH_2CH_3), 5.0 (CH_2CH_3). FT-IR (KBr, cm^{-1}): 2928 (s), 2881 (s), 2800 (m), 1573 (s), 1538 (s), 1491 (m), 1462 (m), 1416 (m), 1402 (m), 1347 (s), 1249 (w), 1230 (w), 1139 (w), 1116 (s), 1058 (m), 1017 (m), 949 (w), 918 (w), 767 (w), 756 (m), 633 (w), 597 (w), 556 (m), 498 (w), 463 (w).

$[Zn(Et)(H\text{-TMG}))(\mu\text{-ONEP})]_2$ (3). H-ONep (0.28 g 3.1 mmol) and **2** (1.9 g 3.1 mmol) in hexanes were used. A solution of H-ONep in hexanes (5 mL) was added dropwise to a stirring solution of **2** in hexanes. The solution was stirred for 15 min and then allowed to sit and evaporate. The compound was subsequently recrystallized from a concentrated hexanes solution at −37 °C to obtain satisfactory elemental analysis. Yield 88% (0.82 g, 2.7 mmol). Mp 76 °C. Anal. Calcd for $C_{24}H_{58}N_6O_2Zn_2$: C, 48.57; H, 9.85; N, 14.16. Found: C, 48.01; H, 10.21; N, 14.48. ^{1}H NMR (400 MHz, toluene-d_8): δ = 5.17 (s, 2H, 2*H*N=CN(CH_3)$_3$), 3.72 (s, 4.0H, 2OC*H*$_2$C-(CH_3)$_3$), 2.65 (s, 18.0H, 2OCH$_2$C(C*H*$_3$)$_3$), 2.33 (s, 24.0H, 2H−N=C(N(C*H*$_3$)$_2$)$_2$), 1.77 (t, 6.0H, 2CH$_2$C*H*$_3$), 0.54 (q, 4.0H, *2CH*$_2$*CH*$_3$). ^{13}C NMR (100.5 MHz, toluene-d_8): δ = 167.8 (HN=*C*(N(CH_3)$_2$)), 78.6 (O*C*H$_2$C(CH_3)$_3$), 39.9 (N=C(N(*C*H_3)$_2$)), 38.9 (*C*H$_2$CH$_3$), 35.0 (OCH$_2$*C*(CH_3)$_3$), 27.9 (OCH$_2$C(*C*H_3)$_3$), 15.3 (CH_2CH_3). FT-IR (KBr, cm^{-1}): 3349 (m), 2947 (s), 2803 (s), 2688 (m), 2639 (m), 1592 (s), 1536 (s), 1459 (s), 1402 (s), 1355 (m), 1281 (m), 1220 (m), 1116 (s), 1085 (s), 1021 (s), 947 (w), 902 (m), 773 (m), 749 (m), 593 (m), 488 (m), 425 (m).

[Zn(Et)(DBP)(H-TMG)] (4). H-DBP (1.3 g, 6.3 mmol), Zn-$(Et)_2$ (4.4 g, 6.3 mmol), H-TMG (0.72 g, 6.3 mmol), and 5 mL of hexane were used. Yield 87% (2.2 g, 5.4 mmol). Mp 113 °C. Anal. Calcd for $C_{21}H_{38}N_3OZn$: C, 60.79; H, 9.47; N, 10.13. Found: C, 60.92; H, 9.70; N, 9.65. ^{1}H NMR (400 MHz, toluene-d_8): δ = 7.35 (m, 1H, OC$_6$*H*$_3$(C(CH_3)$_3$)$_2$), 6.68 (d, 2H, OC$_6$*H*$_3$(C(CH_3)$_3$)$_2$)), 4.38 (s, 1H, *H*N=CN(CH_3)$_3$), 2.28 (s, 6H, HN=*C*(N(C*H*$_3$)$_2$)), 1.85 (s, 6H, HN=*C*(N(C*H*$_3$)$_2$)), 1.71 (s, 18H, OC$_6$H$_3$(C(*CH*$_3$)$_3$)$_2$-2,6), 1.57 (t, 3H, CH$_2$C*H*$_3$), 0.63 (q, 2H, C*H*$_2$CH$_3$). ^{13}C NMR (100.5 MHz, toluene-d_8): δ = 167.1 (HN=*C*(N(CH_3)$_2$)), 138.6, 124.6 113.5,

115.2 ($OC_6H_3(C(CH_3)_3)_2$-2,6), 38.7 ($HN{=}C(N(CH_3)_2)$), 37.6 (OC_6H_3-$(C(CH_3)_3)_2$-2,6), 31.1 ($OC_6H_3(C(CH_3)_3)_2$-2,6), 12.6 (CH_2CH_3), 1.0 (CH_2CH_3). FT-IR (KBr, cm^{-1}): 3362 (w), 2963 (s), 2905 (m), 1577 (m), 1542 (m), 1446 (s), 1412 (m), 1259 (s), 1110 (s), 864 (s), 802 (s), 754 (m), 702 (m), 687 (m), 663 (m), 625 (m), 505 (w).

[Zn(Et)(DBP-4-Me)(H-TMG)] (5). H-DBP-4Me (0.69 g, 3.2 mmol), $Zn(Et)_2$ (2.2 g, 3.2 mmol), H-TMG (0.36 g, 3.2 mmol), and 5 mL of hexanes were used. Yield 97% (1.3 g, 3.1 mmol). Mp 115 °C. Anal. Calcd for $C_{22}H_{41}N_3OZn$: C, 61.60; H, 9.63; N, 9.80. Found: C, 61.14; H, 9.23; N, 9.80. ^{1}H NMR (400 MHz, toluene-d_8): δ = 7.14 (s, 2H, $OC_6H_2(C(CH_3)_3)_2$-2,6-(CH_3)-4), 4.46 (s, 1H, $HN{=}CN(CH_3)_3$), 2.40 (s, 3H, $OC_6H_2(C(CH_3)_3)_2$-2,6-(CH_3)-4), 2.29 (s, 6H, $HN{=}C(N(CH_3)_2)$), 1.87 (s, 6H, $HN{=}C(N(CH_3)_2)$), 1.71 (s, 18H, $OC_6H_2(C(CH_3)_3)_2$-2,6-(CH_3)-4), 1.55 (t, 3H, CH_2CH_3), 0.61 (q, 2H, CH_2CH_3). ^{13}C NMR (100.5 MHz, toluene-d_8): δ = 167.7 ($HN{=}C(N(CH_3)_2)$), 165.3, 138.9, 126.0, 121.4 ($OC_6H_2(C(CH_3)_3)_2$-2,6-(CH_3)-4), 39.4, 38.3 ($HN{=}C(N(CH_3)_2)$), 35.9 ($OC_6H_2(C(CH_3)_3)_2$-2,6-(CH_3)-4), 32.1 ($OC_6H_2(C(CH_3)_3)_2$-2,6-(CH_3)-4), 22.2 (OC_6H_2-$(C(CH_3)_3)_2$-2,6-(CH_3)-4), 13.4 (CH_2CH_3), 1.7 (CH_2CH_3). FT-IR (KBr, cm^{-1}): 3179 (w), 2924 (s), 2852 (s), 2796 (m), 1583 (s), 1547 (m), 1417 (m), 1400 (m), 1339 (m), 1250 (m), 1226 (m), 1141 (m), 1106 (s), 1057 (m), 1012 (m), 948 (w), 917 (m), 759 (m), 627 (m), 599 (m), 553 (m), 499 (w), 457 (w).

[(Zn_2(μ-TMG)(μ-DBP)($Et)_2$] (6). H-DBP (1.29 g, 6.3 mmol), $Zn(Et)_2$ (8.8 g, 12.5 mmol), and H-TMG (0.72 g, 6.3 mmol) were used. Yield 73% (2.2 g, 4.6 mmol). Mp 104 °C. Anal. Calcd for $C_{23}H_{43}N_3OZn_2$: C, 54.34; H, 8.53; N, 8.27. Found: C, 54.57; H, 8.96; N, 8.30. ^{1}H NMR (400 MHz, toluene-d_8): δ = 7.30 (m, 1H, $OC_6H_3(C(CH_3)_3)_2$), 6.79 (d, 2H, $OC_6H_3(C(CH_3)_3)_2$-2,6), 2.46 (s, 12H, $N{=}C(N(CH_3)_2)_2$), 1.63 (s, 18H, $OC_6H_3(C(CH_3)_3)_2$-2,6), 1.25 (t, 3H, CH_2CH_3), 0.51 (q, 2H, CH_2CH_3). ^{13}C NMR (100.5 MHz, toluene-d_8): δ = 160.7 ($N{=}C(N(CH_3)_2)$), 139.8, 126.1, 118.5, 115.9 ($OC_6H_3(C(CH_3)_3)_2$), 39.6 ($N{=}C(N(CH_3)_2)$), 35.7 ($OC_6H_3(C(CH_3)_3)_2$-2,6), 33.2 ($OC_6H_3(C(CH_3)_3)_2$-2,6), 12.8 (CH_2CH_3), 3.5 (CH_2CH_3). FT-IR (KBr, cm^{-1}): 2963 (s), 2905 (m), 1944 (w), 1574 (w), 1446 (w), 1413 (m), 1261 (s), 1020 (s), 864 (m), 798 (m), 702 (m), 503 (w), 405 (w).

[Zn(μ-OCH_3)(DBP-4Me)(H-TMG)]$_2$*2(THF) (7). H-DBP-4Me (0.69 g, 3.1 mmol), $Zn(Et)_2$ (2.2 g, 3.1 mmol), H-TMG (0.36 g, 3.1 mmol), and MeOH (0.10 g, 3.1 mmol) were used. Yield 75% (1.3 g, 1.2 mmol). Mp 188 °C. Anal. Calcd for $C_{50}H_{94}N_6O_6Zn_2$: C, 59.69; H, 9.42; N, 8.35. Found: C, 59.27; H, 9.22; N, 8.38. ^{1}H NMR (400 MHz, THF-d_8): δ = 7.16 (s, 2H, $OC_6H_2(C(CH_3)_3)_2$-2,6-(CH_3)-4), 3.99 (s, 1H, $HN{=}CN(CH_3)_3$), 3.80 (s, 3H, OCH_3), 2.70 (s, 6H, $HN{=}C(N(CH_3)_2)$), 2.51 (s, 3H, $OC_6H_2(C(CH_3)_3)_2$-2,6-(CH_3)-4), 1.84 (s, 6H, $HN{=}C(N(CH_3)_2)$), 1.74 (s, 18H, OC_6H_2-$(C(CH_3)_3)_2$-2,6-(CH_3)-4). ^{13}C NMR (100.5 MHz, THF-d_8): δ = 168.0 ($HN{=}C(N(CH_3)_2)$), 165.6, 139.3, 125.3, 120.7 (OC_6H_2-$(C(CH_3)_3)_2$-2,6-(CH_3)-4), 54.6 (OCH_3), 39.5 ($HN{=}C(N(CH_3)_2)$), 35.6 ($OC_6H_2(C(CH_3)_3)_2$-2,6-(CH_3)-4), 31.3 ($OC_6H_2(C(CH_3)_3)_2$-2,6-(CH_3)-4), 21.2 ($OC_6H_2(C(CH_3)_3)_2$-2,6-(CH_3)-4). FT-IR (KBr, cm^{-1}): 3335 (s), 2950 (s), 2802 (m), 1581 (s), 1415 (s), 1309 (m), 1255 (s), 1129 (s), 1063 (s), 935 (w), 894 (m), 856 (w), 801 (s), 749 (s), 599 (w), 523 (w), 458 (s), 406 (w).

[Zn(μ-OEt)(DBP-4-Me)(H-TMG)]$_2$ (8). H-DBP-4-Me (0.69 g, 3.1 mmol), $Zn(Et)_2$ (2.2 g, 3.1 mmol), H-TMG (0.36 g, 3.1 mmol), and EtOH (0.14 g, 3.2 mmol) were used. Yield 89% (1.2 g, 1.4 mmol). Mp 156 °C. Anal. Calcd for $C_{44}H_{82}N_6O_4Zn_2$: C, 59.38; H, 9.29; N, 9.44. Found: C, 59.00; H, 9.31; N, 9.41. ^{1}H NMR (400 MHz, toluene-d_8): δ = 7.18 (s, 2H, $OC_6H_2(C(CH_3)_3)_2$-2,6-(CH_3)-4), 4.38 (s, 1H, $HN{=}CN(CH_3)_3$), 4.25 (q, 2H, OCH_2CH_3), 2.66 (s, 6H, $HN{=}C(N(CH_3)_2)$), 2.40 (s, 3H, $OC_6H_2(C(CH_3)_3)_2$-2,6-(CH_3)-4), 1.93 (s, 6H, $HN{=}C(N(CH_3)_2)$), 1.73 (s, 18H, $OC_6H_2(C(CH_3)_3)_2$-2,6-(CH_3)-4), 1.28 (t, 3H, OCH_2CH_3). ^{13}C NMR (100.5 MHz, toluene-d_8): δ = 166.7 ($HN{=}C(N(CH_3)_2)$), 164.6, 138.3, 125.3, 120.4 ($OC_6H_2(C(CH_3)_3)_2$-2,6-(CH_3)-4), 60.5 (OCH_2CH_3), 38.8 ($HN{=}C(N(CH_3)_2)$), 35.4 ($OC_6H_2(C(CH_3)_3)_2$-2,6-(CH_3)-4), 31.5 ($OC_6H_2(C(CH_3)_3)_2$-2,6-(CH_3)-4), 21.3 ($OC_6H_2(C(CH_3)_3)_2$-2,6-(CH_3)-4), 21.0 (OCH_2CH_3). FT-IR (KBr, cm^{-1}): 3362 (m), 3337 (m), 2957 (s), 1577 (s), 1541 (s), 1457 (m), 417 (s), 1382 (m), 1262 (s) 1219 (w), 1128 (s), 1100 (s), 1056 (s), 889 (m), 859 (m), 803 (s), 762 (w), 723 (w), 603 (w), 557 (w), 517 (m), 441 (m).

[Zn(μ-OEt)(DBP)(H-TMG)]$_2$ (9). H-DBP (2.2 g, 3.2 mmol), $Zn(Et)_2$ (2.2 g, 3.2 mmol), H-TMG (0.36 g, 3.2 mmol), and EtOH (0.14 g, 3.2 mmol) were used. Yield 99% (1.3 g, 1.6 mmol). Mp 165 °C. Anal. Calcd for $C_{42}H_{78}N_6O_4Zn_2$: C, 58.53; H, 9.12; N, 9.75. Found: C, 58.57; H, 9.25; N, 9.13. ^{1}H NMR (400 MHz, THF-d_8): δ = 7.07 (m, 2H, $OC_6H_3(C(CH_3)_3)_2$-2,6), 6.92 (d, 2H, OC_6H_3-$(C(CH_3)_3)_2$-2,6), 4.26 (s, 1H, $HN{=}CN(CH_3)_3$), 3.91 (q, 2H, OCH_2CH_3), 2.92 (s, 6H, $HN{=}C(N(CH_3)_2)$), 2.50 (s, 6H, $HN{=}C(N(CH_3)_2)$), 1.44 (s, 18H, $OC_6H_3(C(CH_3)_3)_2$-2,6), 1.04 (t, 2H, OCH_2CH_3). ^{13}C NMR (100.5 MHz, THF-d_8): δ = 167.5 ($HN{=}C(N(CH_3)_2)$), 139.7, 138.2, 125.5, 125.1 ($OC_6H_3(C(CH_3)_3)_2$-2,6), 61.4 (OCH_2CH_3), 39.9 ($HN{=}C(N(CH_3)_2)$), 37.8 ($OC_6H_3(C(CH_3)_3)_2$-2,6), 32.1 ($OC_6H_3(C(CH_3)_3)_2$-2,6), 21.6 (OCH_2CH_3). FT-IR (KBr, cm^{-1}): 3365 (m), 2949 (s), 2803 (w), 1572 (s), 1541 (s), 1458 (m), 1404 (s), 1379 (s), 1348 (m), 1324 (w), 1306 (w), 1268 (s), 1202 (m), 1128 (m), 1099 (s), 1059 (m), 1032 (s), 892 (m), 861 (m), 817 (m), 742 (s), 717 (m), 643 (w), 599 (w), 558 (w), 491 (m), 439 (m).

Polymerization Procedure. Under an argon atmosphere, complex **8** was reacted with *rac*-lactide (LA) ([LA]:[cat] = 200) in a Schlenk flask charged with dichloromethane. The reaction was stirred for 24 h and then quenched with methanol. A white polymer resulted after removing the solvent. The resulting polymer was analyzed by ^{1}H and ^{13}C NMR spectroscopy and MALDI-TOF mass spectrometry (Figures 9 and S3).

X-ray Crystal Structure Information. X-ray crystallography was performed by mounting each crystal onto a thin glass fiber from a pool of Fluorolube and immediately placing it under a 100 K N_2 stream, on a Bruker AXS diffractometer. The radiation used was graphite monochromatized Mo Kα radiation (λ = 0.7107 Å). The lattice parameters were optimized from a least-squares calculation on carefully centered reflections. Lattice determination, data collection, structure refinement, scaling, and data reduction were carried out using APEX2 version 1.0-27 software package.

Each structure was solved using direct methods. This procedure yielded the Zn atoms, along with a number of the C, N, and O atoms. Subsequent Fourier synthesis yielded the remaining atom positions. The hydrogen atoms were fixed in positions of ideal geometry and refined within the XSHELL software. These idealized hydrogen atoms had their isotropic temperature factors fixed at 1.2 or 1.5 times the equivalent isotropic U of the C atoms to which they were bonded. The final refinement of each compound included anisotropic thermal parameters on all non-hydrogen atoms. Data collection parameters are listed in Tables 1−3. Interatomic distances and angles are listed in Tables 4−6. Additional information concerning the data collection and final structural solutions of compounds **1**−**9** can be found in the Supporting Information. Any variations from standard structural solution associated with the representative compounds are discussed below.

Results and Discussion

General Considerations. The syntheses of complexes **1**−**9** were performed under an argon atmosphere with the objective of outlining the reactivity of H-TMG with Et_2Zn. All compounds were isolated as colorless crystalline compounds in good yield. **1**−**9** were moderately to slightly soluble in hexanes and readily soluble in THF.

Synthesis. The syntheses of **1** and **2** are shown in Scheme 1. In a hexane solution, the straightforward reaction of 3 or 4 equiv of 1,1,3,3-tetramethylguanidine (H-TMG) with 3 equiv of diethyl zinc results in the immediate evolution of CH_3CH_3.

Table 1. Data Collection Parameters for 1−3

	compound		
	1	**2**	**3**
chemical formula	$C_{24}H_{58}N_{12}Zn_3$	$C_{21}H_{51}N_9Zn_3$	$C_{24}H_{58}N_6O_2Zn_2$
formula weight	710.93	625.82	593.50
temp (K)	100(2)	100(2)	100(2)
space group	monoclinic *P*2(1)/*n*	triclinic *P*-1	triclinic *P*-1
a (Å)	13.5902(13)	10.083(2)	9.5136(17)
b (Å)	14.3845(13)	11.379(2)	9.9491(18)
c (Å)	18.5827(17)	13.732(3)	10.1261(18)
α (deg)		92.734(4)	117.446(3)
β (deg)	101.762(2)	99.931(4)	98.305(3)
γ (deg)		99.860(4)	94.292(3)
V (Å^3)	3556.4(6)	1524.0(5)	830.7(3)
Z	4	2	1
D_{calcd} (Mg/m^3)	1.328	1.364	1.186
μ (Mo Kα) (mm^{-1})	2.039	2.366	1.470
R1[a] (%) (all data)	5.59 (13.84)	4.51 (5.89)	3.23 (4.66)
wR2[b] (%) (all data)	12.16 (15.88)	11.88 (12.95)	8.92 (10.26)

[a] $R1 = \sum||F_o| - |F_c||/\sum|F_o| \times 100$. [b] $wR2 = [\sum w(F_o^2 - F_c^2)^2/\sum(w|F_o|^2)^2]^{1/2} \times 100$.

Table 2. Data Collection Parameters for 4−6

	compound		
	4	**5**	**6**
chemical formula	$C_{21}H_{39}N_3OZn$	$C_{22}H_{41}N_3OZn$	$C_{23}H_{43}N_3OZn_2$
formula weight	414.92	428.95	508.34
temp (K)	100(2)	100(2)	188(2)
space group	monoclinic *P*2(1)/*n*	monoclinic *P*2(1)/*c*	monoclinic *P*2(1)
a (Å)	11.186(2)	9.2716(5)	10.4473(9)
b (Å)	13.866(3)	12.0066(8)	17.4330(14)
c (Å)	15.376(3)	21.7463(14)	14.5079(12)
α (deg)			
β (deg)	99.819(4)	94.9850(10)	90.339(2)
γ (deg)			
V (Å^3)	2349.9(8)	2411.6(3)	2642.2(4)
Z	4	4	4
D_{calcd} (Mg/m^3)	1.173	1.181	1.278
μ (Mo Kα) (mm^{-1})	1.058	1.033	1.832
R1[a] (%) (all data)	5.67 (12.41)	4.97 (7.52)	4.18 (7.10)
wR2[b] (%) (all data)	13.82 (18.81)	7.54 (7.88)	7.96 (8.38)

[a] $R1 = \sum||F_o| - |F_c||/\sum|F_o| \times 100$. [b] $wR2 = [\sum w(F_o^2 - F_c^2)^2/\sum(w|F_o|^2)^2]^{1/2} \times 100$.

Table 3. Data Collection Parameters for 7−9

	compound		
	7	**8**	**9**
chemical formula	$C_{50}H_{94}N_6O_6Zn_2$	$C_{44}H_{82}N_6O_4Zn_2$	$C_{42}H_{78}N_6O_4Zn_2$
formula weight	1006.05	89.90	861.84
temp (K)	100(2)	100(2)	100(2)
space group	triclinic *P*-1	monoclinic *P*2(1)/*c*	triclinic *P*-1
a (Å)	9.2885(13)	10.2512(17)	9.5000(14)
b (Å)	9.6888(13)	16.578(3)	9.805(2)
c (Å)	16.675(2)	14.609(3)	14.350(2)
α (deg)	84.828(2)		71.257(6)
β (deg)	80.272(2)	91.008(4)	79.161(17)
γ (deg)	66.688(2)		64.983(9)
V (Å^3)	1357.9(3)	2482.2(7)	1144.9(3)
Z	1	2	1
D_{calcd} (Mg/m^3)	1.230	1.191	1.250
μ (Mo Kα) (mm^{-1})	0.933	1.009	1.092
R1[a] (%) (all data)	3.71 (5.42)	4.15 (7.85)	4.08 (6.43)
wR2[b] (%) (all data)	10.35 (12.32)	10.90 (13.82)	10.47 (12.17)

[a] $R1 = \sum||F_o| - |F_c||/\sum|F_o| \times 100$. [b] $wR2 = [\sum w(F_o^2 - F_c^2)^2/\sum(w|F_o|^2)^2]^{1/2} \times 100$.

Reducing the solutions to dryness provides colorless crystals of $[Zn_3(\mu\text{-TMG})_4(Et)_2]$ (**1**) and $[Zn(\mu\text{-TMG})(Et)]_3$ (**2**), respectively. Both complexes are readily soluble in hydrocarbon solvents. Retention of the zinc-bonded ethyl group for **1** and **2** is implied by the observation of a triplet ($\delta = 1.64$ for **1** and 1.54 for **2**) and a quartet ($\delta = 0.62$ for **1** and 0.47 for **2**) by ^{1}H NMR spectroscopy. FT-IR spectroscopy was utilized to confirm

Table 4. Selected Interatomic Distances (Å) and Angles (deg) for 1 and 2

	Complex **1**		
Zn(1)−N(4)	1.995(6)	Zn(1)−N(10)	2.021(5)
Zn(1)−N(7)	2.024(5)	Zn(1)−N(1)	2.034(5)
Zn(2)−N(1)	1.964(5)	Zn(2)−N(7)	1.983(5)
Zn(2)−C(21)	1.964(8)	Zn(3)−N(4)	1.976(5)
Zn(3)−N(10)	1.978(5)	Zn(3)−C(23)	1.981(10)
N(1)−C(1)	1.285(8)	N(2)−C(1)	1.394(8)
N(3)−C(1)	1.373(8)		
N(4)−Zn(1)−N(7)	122.9(2)	N(4)−Zn(1)−N(10)	85.9(2)
N(7)−Zn(1)−N(10)	122.7(2)	N(4)−Zn(1)−N(1)	121.9(2)
N(7)−Zn(1)−N(1)	85.9(2)	N(10)−Zn(1)−N(1)	122.1(2)
N(1)−Zn(2)−C(21)	135.4(3)	N(1)−Zn(2)−N(7)	89.0(2)
C(21)−Zn(2)−N(7)	132.7(3)	N(4)−Zn(3)−N(10)	87.6(2)
N(4)−Zn(3)−C(23)	137.7(4)	N(10)−Zn(3)−C(23)	133.2(4)
Zn(2)−N(1)−Zn(1)	90.5(2)	Zn(3)−N(4)−Zn(1)	91.5(2)
Zn(2)−N(7)−Zn(1)	90.2(2)	Zn(3)−N(10)−Zn(1)	90.7(2)
	Complex **2**		
Zn(1)−N(7)	1.960(2)	Zn(1)−C(1)	1.983(3)
Zn(1)−N(1)	2.021(2)	Zn(2)−C(3)	1.984(3)
Zn(2)−N(4)	1.984(2)	Zn(2)−N(7)	1.998(2)
Zn(3)−N(4)	1.978(2)	Zn(3)−C(5)	1.987(3)
Zn(3)−N(1)	2.001(2)	N(3)−C(7)	1.390(4)
N(1)−C(7)	1.278(4)	N(2)−C(7)	1.414(4)
N(7)−Zn(1)−C(1)	133.46(14)	N(7)−Zn(1)−N(1)	99.62(10)
C(1)−Zn(1)−N(1)	124.89(14)	C(3)−Zn(2)−N(4)	134.74(13)
C(3)−Zn(2)−N(7)	120.13(13)	N(4)−Zn(2)−N(7)	105.09(10)
N(4)−Zn(3)−C(5)	130.76(12)	N(4)−Zn(3)−N(1)	97.60(9)
C(5)−Zn(3)−N(1)	131.40(12)	Zn(3)−N(1)−Zn(1)	101.43(10)
Zn(3)−N(4)−Zn(2)	104.72(11)	Zn(1)−N(7)−Zn(2)	101.81(11)

Table 5. Selected Interatomic Distances (Å) and Angles (deg) for 3−6

	Complex **3**		
Zn(1)−O(1)	2.0152(19)	Zn(1)−N(1)	2.074(2)
Zn(1)−O(1A)	2.0200(19)	Zn(1)−C(11)	1.996(3)
N(1)−C(6)	1.299(4)	N(2)−C(6)	1.361(4)
N(3)−C(6)	1.376(4)		
C(11)−Zn(1)−O(1)	122.18(11)	O(1)−Zn(1)−O(1A)	84.75(8)
C(11)−Zn(1)−N(1)	128.00(12)	O(1)−Zn(1)−N(1)	97.06(9)
O(1A)−Zn(1)−N(1)	87.76(9)	C(1)−O(1)−Zn(1)	121.01(17)
Zn(1)−O(1)−Zn(1A)	95.25(7)		
	Complex **4**		
Zn(1)−O(1)	1.900(3)	Zn(1)−C(20)	1.943(6)
Zn(1)−N(1)	1.957(5)	N(1)−C(15)	1.327(7)
N(2)−C(15)	1.349(6)	N(3)−C(15)	1.348(7)
O(1)−Zn(1)−C(20)	135.7(2)	C(20)−Zn(1)−N(1)	134.2(3)
O(1)−Zn(1)−N(1)	90.04(17)	C(1)−O(1)−Zn(1)	141.6(3)
	Complex **5**		
Zn(1)−O(1)	1.9075(19)	Zn(1)−C(21)	1.965(4)
Zn(1)−N(1)	1.961(2)	N(1)−C(16)	1.311(3)
N(2)−C(16)	1.359(3)	N(3)−C(16)	1.362(4)
O(1)−Zn(1)−C(21)	132.37(13)	O(1)−Zn(1)−N(1)	88.24(9)
C(21)−Zn(1)−N(1)	139.26(13)	C(1)−O(1)−Zn(1)	128.49(17)
	Complex **6**		
Zn(1)−C(20)	1.929(6)	Zn(1)−N(1)	1.926(5)
Zn(1)−O(1)	2.038(3)	Zn(2)−N(1)	1.909(4)
Zn(2)−C(22)	1.958(9)	Zn(2)−O(1)	2.079(4)
N(1)−C(15)	1.313(7)	N(2)−C(15)	1.361(7)
N(3)−C(15)	1.367(7)		
C(20)−Zn(1)−N(1)	146.6(2)	C(20)−Zn(1)−O(1)	128.8(2)
N(1)−Zn(1)−O(1)	83.65(17)	N(1)−Zn(2)−C(22)	147.2(4)
N(1)−Zn(2)−O(1)	82.97(16)	C(22)−Zn(2)−O(1)	129.8(4)
Zn(2)−N(1)−Zn(1)	101.2(2)	Zn(1)−O(1)−Zn(2)	92.05(14)

Table 6. Selected Interatomic Distances (Å) and Angles (deg) for 7−9

	Complex **7**		
Zn(1)−O(1)	1.9316(18)	Zn(1)−O(2A)	1.9795(19)
Zn(1)−O(2)	1.9743(19)	Zn(1)−N(1)	1.985(2)
O(2)−Zn(1A)	1.9795(19)		
O(1)−Zn(1)−O(2)	111.44(8)	O(1)−Zn(1)−O(2A)	122.01(8)
O(2)−Zn(1)−O(2A)	82.80(8)	O(1)−Zn(1)−N(1)	104.73(9)
O(2)−Zn(1)−N(1)	123.76(9)	O(2A)−Zn(1)−N(1)	112.37(9)
Zn(1)−O(2)−Zn(1A)	97.20(8)		
	Complex **8**		
Zn(1)−O(1)	1.926(2)	Zn(1)−O(2)	1.967(2)
Zn(1)−O(2A)	1.975(2)	Zn(1)−N(1)	1.988(3)
N(1)−C(18)	1.309(4)	N(2)−C(18)	1.355(5)
N(3)−C(18)	1.363(5)		
O(1)−Zn(1)−O(2)	122.16(10)	O(1)−Zn(1)−O(2A)	113.90(10)
O(2)−Zn(1)−O(2A)	81.79(11)	O(1)−Zn(1)−N(1)	101.37(12)
O(2)−Zn(1)−N(1)	117.91(11)	O(2A)−Zn(1)−N(1)	120.49(13)
Zn(1)−O(2)−Zn(1A)	98.21(11)	C(1)−O(1)−Zn(1)	132.9(2)
C(16)−O(2)−Zn(1)	129.4(2)		
	Complex **9**		
Zn(1)−O(1)	1.935(2)	Zn(1)−O(3A)	1.971(2)
Zn(1)−O(3)	1.972(2)	Zn(1)−N(1)	1.990(3)
O(3)−Zn(1A)	1.971(2)	N(1)−C(15)	1.314(4)
N(2)−C(15)	1.356(4)	N(3)−C(15)	1.357(4)
O(1)−Zn(1)−O(3A)	112.12(9)	O(3A)−Zn(1)−O(3)	81.58(9)
O(1)−Zn(1)−O(3)	123.05(10)	O(1)−Zn(1)−N(1)	101.75(10)
O(3A)−Zn(1)−N(1)	124.86(11)	O(3)−Zn(1)−N(1)	114.63(10)
Zn(1A)−O(3)−Zn(1)	98.42(9)	C(1)−O(1)−Zn(1)	136.24(19)
C(20)−O(3)−Zn(1)	127.29(19)		

the υ(C═N) of absorption bands around 1550 cm^{-1} corresponding to the N_{imino} coordinated to zinc.

The reactions shown in Scheme 2 were followed for the synthesis of the novel family of "Zn(Et)(OR)(H-TMG)" compounds (**3**−**5**). To synthesize **3**−**5**, complex **2** was dissolved in hexane and allowed to react with the respective H-OR for an hour. For each derivative, a precipitate formed that dissolved upon heating the solution. Colorless crystals were grown by allowing the reaction mixtures to cool and slowly evaporate or by cooling the reaction mixture (−37 °C). FT-IR spectroscopy on **3**−**5** confirmed absorption bands corresponding to υ(N−H) and υ(C═N) stretching modes around 3100 and 1580 cm^{-1}, respectively. **3**−**5** show no OH peaks around 3000 cm^{-1}, which is consistent with full exchange. For the Zn−O interactions, there should be a stretch present between 800 and 400 cm^{-1}. For each sample, a stretch around 755 cm^{-1} was observed, which is tentatively assigned to the Zn−O. ^{1}H and ^{13}C NMR spectroscopy were once again utilized to confirm retention of the zinc-bonded ethyl groups for **3**−**5**.

The reaction of Et_2Zn with complex **4** in hexanes results in the rapid evolution of CH_3CH_3 (see Scheme 2). Evaporation of the solvent resulted in the isolation of [(Zn_2(μ-TMG)(μ-DBP)-$(Et)_2$] (**6**) as colorless crystals in good yield. ^{1}H NMR spectroscopy for **6** confirmed the existence of the zinc-bonded ethyl group by the observation of a triplet (δ = 1.64) and a quartet (δ = 0.62). FT-IR spectroscopy on **6** confirms absorption bands corresponding to υ(C═N) band at 1546 cm^{-1}. In addition, the spectrum for **6** exhibits no N−H peaks around 3100 cm^{-1}, which is consistent with full exchange. For the Zn−O interactions, a stretch at 754 cm^{-1} was observed, which is tentatively assigned to the Zn−O interaction.

The syntheses of **7**−**9** are shown in Scheme 3. For each reaction, "Zn(Et)(OR)(H-TMG)" was dissolved in hexanes and allowed to react with H-OR′ (OR′ = OMe or OEt). CH_3CH_3 evolved, and a precipitate formed that would not dissolve even upon heating. THF was added, and the reaction was heated again until each reaction went clear. Notably, the DBP-4Me derivatives (**7** and **8**) demonstrated increased solubility in hexanes and toluene versus compound **9**. Crystals of **7**−**9** were grown by allowing their respective reaction mixtures to cool and slowly evaporate. ^{1}H and ^{13}C NMR spectroscopy were utilized to confirm the presence of OR′ (OR′ = OMe or OEt) for **7**−**9**. FT-IR spectroscopy on **7**−**9** confirmed absorption bands corresponding to υ(N−H) and υ(C═N) stretching modes around 3100 and 1580 cm^{-1}, respectively.

Structural Descriptions. [Zn_3(μ-TMG)$_4$($Et)_2$] (1). The thermal ellipsoid plot of compound **1** is illustrated in Figure 1. **1** is perhaps best compared to the previously reported Zn phosphoraneiminato complex, [Zn_3(μ-N═PMe_3)$_4${$N(SiMe_3)_2$}$_2$].[10] The structure consists of a nonlinear array of three metal atoms (Zn···Zn···Zn = 164.17°) that are bridged by four TMG ligands. The terminal zincs are further coordinated to ethyl groups. The central metal has a distorted tetrahedral geometry, and the two terminal zincs have a trigonal-planar coordination. The Zn−N distances in **1** average 2.011 Å for the central zinc and 1.975 Å for the outer zincs. For the terminal zincs, the average Zn−C distance is 1.972 Å. The C═N imino donors range from 1.264 to 1.284 Å and are typical for a carbon−nitrogen double bond.[7] The other two C−N distances range from 1.372 to 1.412(4) Å, and the interactions of these N atoms with zincs are negligible (the shortest Zn···N distance is 3.406 Å).

[Zn(μ-TMG)(Et)]$_3$ (2). The X-ray crystallographic study of **2** shows it to exist as a cyclic trinuclear complex in the solid state (Figure 2). This is comparable to the cyclic [Zn{μ-P(Cyclohexyl)$_2$}(Et)]$_3$ published by Wright and co-workers.[11] The complex has a chair-shaped Zn_3N_3 hexanuclear core in with Zn−N bonds range from 1.959 to 2.021 Å. The Zn centers have almost identical trigonal planar geometries ($\sum$ of the three angles about Zn average 359.9°). The ring angles at Zn and N are 100.8° (average) for N−Zn−N and 102.7° (average) for Zn−N−Zn. Additionally, all of the zincs are coordinated to ethyl groups with an average Zn−C distance of 1.984 Å.

[Zn(Et)(H-TMG**))(μ-ONEP)]$_2$ (3).** Figure 3 shows the thermal ellipsoid plot of **3**. The structure of **3**, similar to the previously described pyridine adduct [Zn(Et)(py))(μ-ONEP)]$_2$,[12] proved to be a centro-symmetric dinuclear complex wherein each zinc atom is tetrahedrally bound by two bridging neopentoxide ligands, one terminal ethyl group, and one H-TMG ligand. The Zn−O distances in **3** average 2.018 Å, and the Zn−C distances are 1.995 Å. The Zn−N distances of 2.074 Å are consistent with assigning the additional coordination of H-TMG to zinc.

[Zn(Et)(DBP)(H-TMG)] (4) and [Zn(Et)(DBP-4-Me)(H-TMG)] (5). The structures of **4** and **5** are illustrated in the thermal ellipsoid plot of **4** (Figure 4). Both **4** and **5** are examples of neutral monomeric three-coordinate zinc complexes and perhaps best compared to the three-coordinate [Zn(Me)(DBP)-{$Me_2NC(N^iPr)_2$}] described by Coles and co-workers.[13] Each trigonal planar zinc metal center was determined to be coordinated to one aryloxide, one ethyl group, and one H-TMG. The bond lengths (Zn−O, Zn−C, and Zn−N) are very similar for **4** and **5**. A shorter Zn−O diatance (1.900 Å) is observed for **4** and **5** as compared to [Zn(Me)(DBP){$Me_2NC(N^iPr)_2$}] (1.951 Å).[13]

(10) Krieger, M.; Gould, R. O.; Neumuller, B.; Harms, K.; Dehnicke, K. *Z. Anorg. Allg. Chem.* **1998**, *624*, 1434.
(11) Edwards, A. J.; Paver, M. A.; Raithby, P. R.; Russell, C. A.; Wright, D. S. *Organometallics* **1993**, *12*, 4687.
(12) Boyle, T. J.; Bunge, S. D.; Andrews, N. L.; Matzen, L. E.; Sieg, K.; Rodriguez, M. A.; Headley, T. J. *Chem. Mater.* **2004**, *16*, 3279.
(13) Coles, M. P.; Hitchcock, P. B. *Eur. J. Inorg. Chem.* **2004**, 2662.

Scheme 2. Synthesis of 3−6

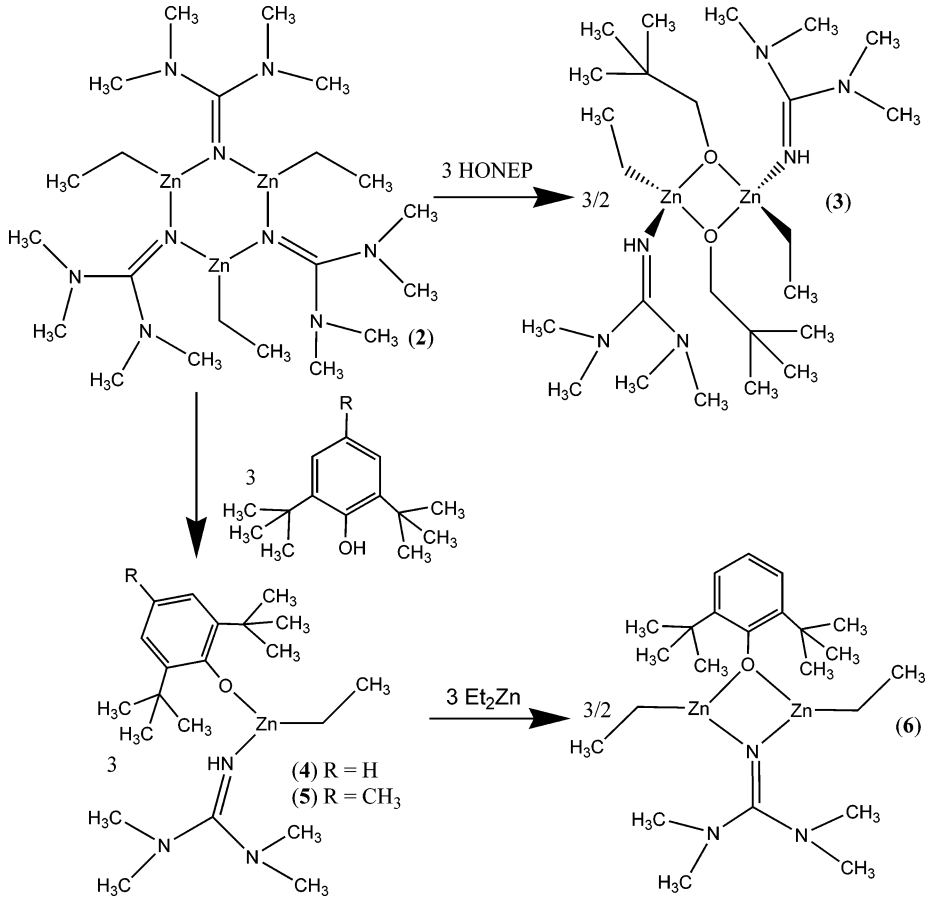

Scheme 3. Synthesis of 7−9

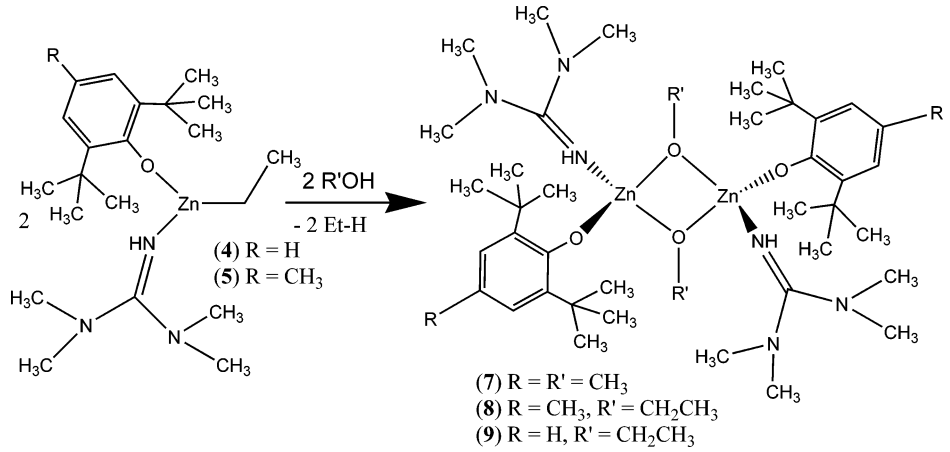

[(Zn$_2$(μ-TMG)(μ-DBP)(Et)$_2$] (6). Compound **6** crystallizes in the monoclinic space group *P*2(1) with two crystallographicly inequivalent, but nearly identical, dinuclear zinc complexes per unit cell. The structure of **6** is depicted in Figure 5. Each trigonal planar zinc atom is bridged to the adjacent zinc via one TMG [Zn−N 1.918 Å (average)] and one aryloxide ligand [Zn−O 2.058 Å (average)]. One ethyl group is additionally coordinated to each metal center [Zn−C 1.944 Å (average)].

[Zn(μ-OCH$_3$)(DBP-4Me)(H-TMG)]$_2$*2(THF) (7), [Zn(μ-OEt)(DBP-4-Me)(H-TMG)]$_2$ (8), and [Zn(μ-OEt)(DBP)(H-TMG)]$_2$ (9). The structures of compounds **7**, **8**, and **9** may be illustrated by the thermal ellipsoid plots of **7** and **8** shown in Figures 6 and 7, respectively. All three complexes have a planar Zn_2O_2 core where each zinc atom is tetrahedrally coordinated by two bridging alkoxide groups, one terminal aryloxide, and one H-TMG ligand. The terminal aryloxide ligands of **7**, **8**, and **9** notably exhibit a small Zn−O−Ar angle, demonstrating the absence of π-donation from the aryl ring, a feature typically found present in early transition metal aryloxide compounds.[14]

PGSE Measurements. To examine whether **7**−**9** exist primarily in solution as a monomer or dinuclear complex, pulsed gradient spin−echo (PGSE) NMR measurements were performed.[15] The PGSE method has been successful at assessing effective hydrodynamic volumes of inorganic complexes in solution through determination of the diffusion coefficient, a number related to the translational motion of a compound in solution.[16] Because of the similarity in size of **5** to the expected

(14) Bradley, D. C.; Mehrotra, R. C.; Rothwell, I. P.; Singh, A. *Alkoxo and Aryloxo Derivatives of Metals*; 2001.

(15) Price, W. S. *Concepts Magn. Reson.* **1997**, *9*, 299.

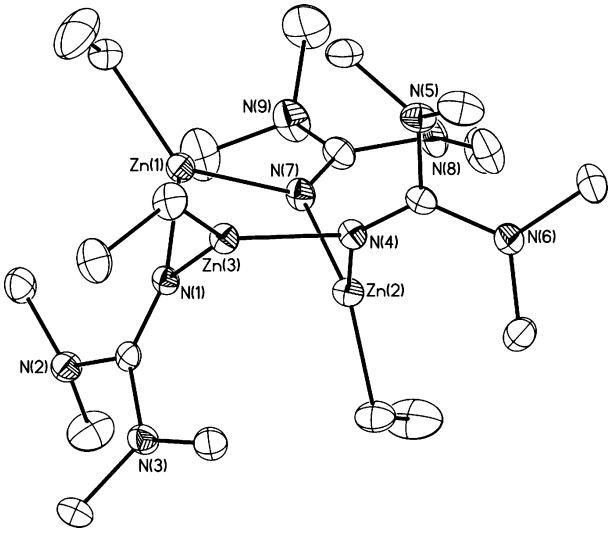

Figure 2. Thermal ellipsoid plot of **2**. Ellipsoids are drawn at the 30% level. H atoms have been omitted for clarity.

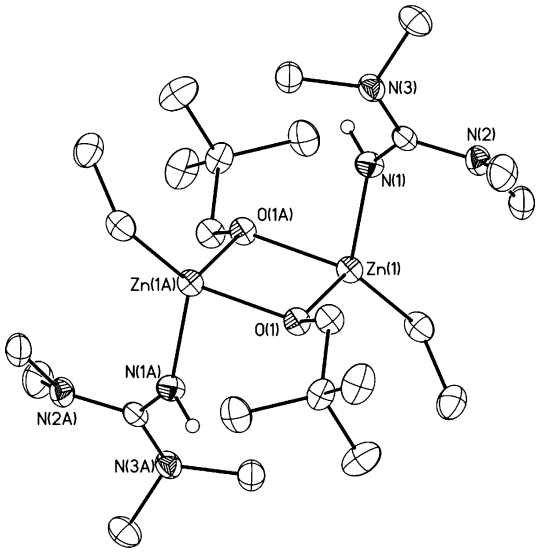

Figure 3. Thermal ellipsoid plot of **3**. Ellipsoids are drawn at the 30% level. H atoms have been omitted for clarity.

monomeric form of **8**, PGSE experiments on d_8-toluene solutions of **8** and **5** were performed. The results are displayed in Figure 8, plotted as $\ln(I/I_0)$ (where I = observed spin−echo intensity and I_0 = intensity in the absence of gradients), versus a function with the square of the gradient strength over a constant diffusion time. Each data point represents an average of the values obtained for the different resonances in the NMR spectrum of each compound at varying gradient strengths. The slopes of the lines in Figure 8 are equal to the diffusion coefficients (D) according to eq 1. The absolute value of the slope decreases with increasing effective hydrodynamic radii according to the Stokes−Einstein eq 2. The experimentally determined values of D and r were calculated and are listed in Table 7. From these data, the effective hydrodynamic volume for **8** was determined to be greater than that for **5**. For comparison, we also estimated values of the molecular radii (r') for **5** and **8** from their X-ray crystal structures by measuring

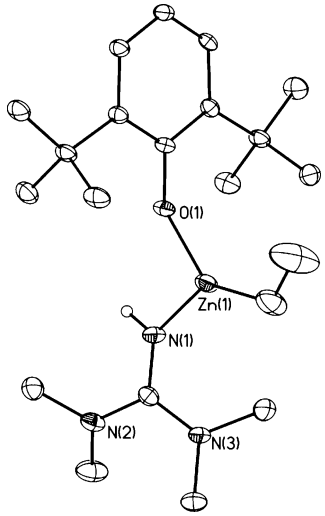

Figure 4. Thermal ellipsoid plot of **4**. Ellipsoids are drawn at the 30% level. H atoms have been omitted for clarity.

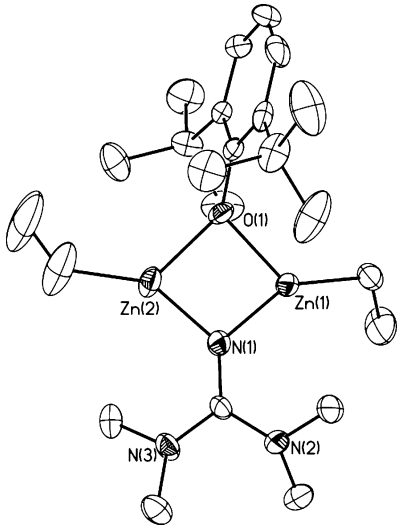

Figure 5. Thermal ellipsoid plot of **6**. Ellipsoids are drawn at the 30% level. H atoms have been omitted for clarity. There are two crystallographically independent, but chemically equivalent, molecules present in the asymmetric unit. One molecule is shown.

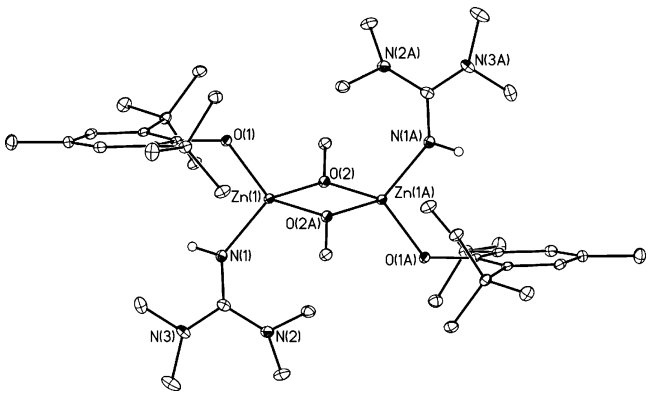

Figure 6. Thermal ellipsoid plot of **7**. Ellipsoids are drawn at the 30% level. H atoms have been omitted for clarity.

the lengths between centers of distant hydrogen atoms on the molecular periphery. All of the complexes were considered as prolate ellipsoids (Table 7), and r' was determined by using eq 3. The values of r (PGSE) and r' (X-ray) for **5** were found to closely agree. In contrast, for **8**, the value of r determined by the PGSE measurement is 28% smaller than the radius estimated

(16) Geldbach, T. J.; Pregosin, P. S.; Albinati, A.; Rominger, F. *Organometallics* **2001**, *20*, 1932. Pichota, A.; Pregosin, P. S.; Valentini, M.; Worle, M.; Seebach, D. *Angew. Chem., Int. Ed.* **2000**, *39*, 153. Mukherjee, R.; Dougan, B. A.; Fry, F. H.; Bunge, S. D.; Ziegler, C. J.; Brasch, N. E. *Inorg. Chem.* **2007**, *46*, 1575.

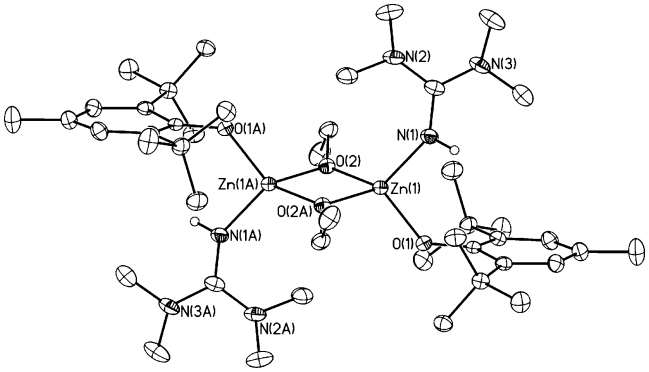

Figure 7. Thermal ellipsoid plot of **8**. Ellipsoids are drawn at the 30% level. H atoms have been omitted for clarity.

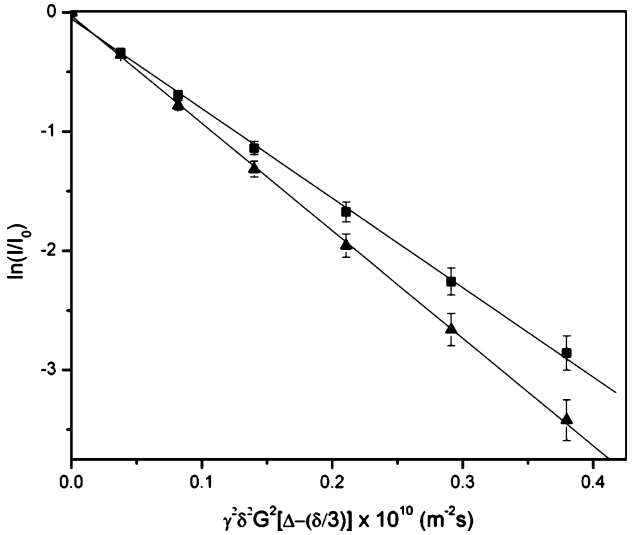

Figure 8. Plot of $\ln(I/I_0)$ versus $\gamma^2\delta^2G^2[\Delta - (\delta/3)] \times 10^{10}$ (m^{-2} s) from PGSE experiments for **5** (■) and **8** (▲).

Table 7. PGSE Experimental Results As Compared to Estimated Data from X-ray Crystal Structures[a]

complex	D[b] ($\times 10^{10}$ m^2 s^{-1})	r[c] (Å)	a[d] (Å)	b[d] (Å)	r'[e] (Å)	D''[b] ($\times 10^{10}$ m^2 s^{-1})
5	9.0(2)	4.0(3)	6.3(7)	3.6(1)	4.3(6)	8.3(4)
8	7.5(1)	4.8(4)	8.9(7)	5.9(2)	6.7(9)	5.3(5)

[a] Estimated errors are indicated in parentheses, with terms defined in the text. [b] From slopes of the lines in Figure 12, eq 1, and eq 2. [c] The errors are estimated to be ~5% primarily on the basis of the accuracy of η used in the calculation. [d] Estimated values from the X-ray crystal structure by measuring the lengths between the centers of distant hydrogen atoms on the periphery corresponding to each arbitrary axis and by calculating the minimum ellipsoid into which the molecule fits. [e] Calculated using eq 3. Equation 3: $r' = (ab^2)^{1/3}$. Equation 2: $D = kT/(6\pi\eta r)$. Equation 1: $\ln(I/I_0) = -\gamma^2\delta^2G^2(\Delta - \delta/3)D$ (G = gradient strength, γ = gyromagnetic ratio, δ = length of gradient pulse, Δ = delay between gradient midpoints, r = effective hydrodynamic radius, and η = viscosity).

from the X-ray crystal structure (r') of the dinuclear form. These data strongly suggest that **8** does not retain its dinuclear form in solution. We also calculated diffusion coefficients (D') from the values of a, b, and r', which required the use of a variant of eq 2 appropriate for prolate ellipsoids. As expected, the agreement between the PGSE measured (D) and predicted (D') diffusion coefficients is excellent for **5** (consistent with the agreement of r and r'), but D' for **8** is much less than the measured value, again consistent with the form of **8** in solution being significantly smaller than the dinuclear structure adopted in the crystal. On this basis, therefore, one can suggest that **8** is predominantly a monomer in d_8-toluene. To confirm this

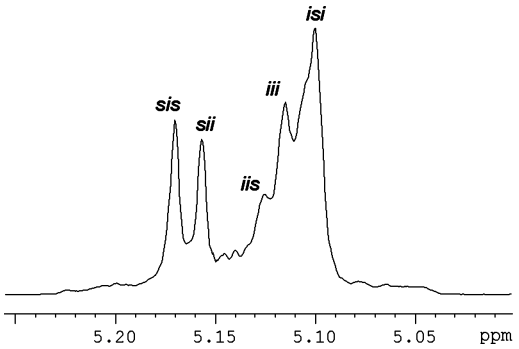

Figure 9. ^{1}H NMR spectra (400 MHz, $CDCl_3$) of PLA methine resonances with selective decoupling of PLA methyl resonances.

suggestion, one can further estimate an upper bound for the radius expected for the monomeric **8**, $r' = 5.1$ Å, by adding approximately one-half of the distance of an O−Et bond (0.7 Å) to the r' value for **5** (4.4 Å). This estimated r' was then used to calculate $D' = 7.1 \times 10^{-10}$ m^2 s^{-1} (assuming a spherical shape for the molecule). Both the estimated r' and D' values for the supposed monomeric form closely agree with those that were experimentally determined for **8**. Therefore, we can conclude **8** has a monomeric structure in solution.

***rac*-Lactide Polymerization.** Both organic and inorganic catalysts have been reported for the ring-opening polymerization of lactide (LA).[3,13,17,18] In fact, a number of elegant syntheses utilizing Zn alkoxides supported by tris(pyrazolyl)hydroborate or β-diketiminate ligands have been performed and were found to produce quite active and, in some cases, stereoselective polymerization catalysts.[2,18,19] The structures of **7**−**9** resemble recently reported active Zn catalysts.[20] Inspired by this resemblance, we explored the capability of **8** to polymerize *rac*-LA. It should be noted that there are at least two possible problems with this approach: disassociation of both H-TMG and/or aryloxide ligands resulting in the formation of ill-defined catalytic species. However, preliminary results have demonstrated neither of these issues to be a problem. In fact, Zn complexes coordinated with H-TMG are crystallized from THF with no THF found coordinated to the metal center. In all of our studies, there has been no evidence that H-TMG disassociates from the metal in favor of coordinating another Lewis base. As for the potential reactivity of the aryloxide ligand, its disassociation is tempered by its interaction with the H-TMG moiety, the steric bulk located on the ring, and also the utilization of a highly reactive alkoxide substituent (OR′) on the metal center.

8 was reacted with *rac*-lactide (LA) ([LA]:[cat] = 200) in dichloromethane for 1 day and then quenched with methanol. A white polymer resulted after removing the solvent. The resultant polymer was examined by ^{1}H NMR spectroscopy (M_n = 24.7 kg mol^{-1}), and the tacticity was investigated by examination of the PLA methine resonances with selective decoupling of PLA methyl resonances (Figure 9). The percent of heterotactic tetrads (*isi* and *sis*) indicates a low degree of heterotacticity. The resultant polymer was further examined with MALDI-TOF mass spectrometry (Figure S3). The spectrum

(17) Myers, M.; Connor, E. F.; Glauser, T.; Mock, A.; Nyce, G.; Hedrick, J. L. *J. Polym. Sci., Part A: Polym. Chem.* **2002**, *40*, 844.
(18) C0hisholm, M. H.; Eilerts, N. W.; Huffman, J. C.; Iyer, S. S.; Pacold, M.; Phomphrai, K. *J. Am. Chem. Soc.* **2000**, *122*, 11845.
(19) Chamberlain, B. M.; Cheng, M.; Moore, D. R.; Ovitt, T. M.; Lobkovsky, E. B.; Coates, G. W. *J. Am. Chem. Soc.* **2001**, *123*, 3229.
(20) Williams, C. K.; Breyfogle, L. E.; Choi, S. K.; Nam, W.; Young, V. G.; Hillmyer, M. A.; Tolman, W. B. *J. Am. Chem. Soc.* **2003**, *125*, 11350.

indicates polymer with little cyclic ether formation, and also little transesterification.

Discussion

The synthesis of **1**−**9** was accomplished via the straightforward reaction of diethyl zinc with various ratios of guanidine and alcohol. The volatility of the ethane side product typically serves to drive the forward reaction and thus facilitate nearly quantitative yield. Following this approach resulted in the clean formation of the guanidinate complexes **1** and **2**. The formation of relatively strong Zn−N and C−H bonds, at the expense of breaking the N−H and a relatively weak Zn−C bond, ensures favorable reaction energies.

Further reaction of **2** with an additional equivalent of alcohol resulted in the isolation of the hetero-ligated complexes **3**−**5**. For this series of reactions, protonation of the guanidinate ligand and the formation of a Zn−O bond were energetically preferred versus breaking an additional Zn−C bond, forming a C−H bond and liberating ethane. This stepwise reactivity is without precedent in organo-zinc chemistry.

The reactivity of H-TMG coordinated to Zn was examined via the reaction of **4** with a stoichiometric equivalent of diethyl zinc. Deprotonation of the coordinated H-TMG and the liberation of ethane resulted in the formation of the dinuclear complex **6**. In **6**, each trigonal planar Zn is connected to the adjacent Zn via bridging TMG and aryloxide ligands. The Zn atoms are further coordinated to terminal ethyl substituents. This remarkably "simple" low-coordinate Zn_2NO ring is without structural precedent. It is noteworthy that preliminary studies of the reactivity of **6** with alcohols were performed and the dinuclear Zn core was found to not be retained. Instead, a mixture of Zn-containing products is formed.

The synthesis of **7**, **8**, and **9** was performed by reacting **4** and **5** with either methanol or ethanol. Ethane is readily liberated, and the corresponding dinuclear Zn alkoxide is isolated in good yield. For complexes **7**−**9**, the tetrahedral Zn atom is coordinated to a terminal aryloxide, H-TMG, and is connected to the other Zn via two bridging alkoxide ligands. These complexes resemble the recently reported dinuclear Zn alkoxide complexes with general formula $[Zn(\mu\text{-OR})(L)]_2$ reported by Tolman and co-workers.[20] These reported Zn complexes demonstrated potential for use as polymerization catalysts. We therefore demonstrated that **8** exists as a monomer in solution and is an active catalyst for the ring-opening polymerization of *rac*-LA to PLA.

Summary and Conclusion

We have successfully synthesized and characterized a series of novel guanidinate- and guanidine-stabilized Zn compounds. The complexes were characterized through use of single-crystal X-ray diffraction, elemental analysis, FT-IR, and ^1H and ^{13}C NMR. The reactions took place stoichiometrically producing mononuclear, dinuclear, or trinuclear compounds. Compound **8** was found to be a monomer in solution and successfully catalyzed the ring-opening polymerization of *rac*-lactide into poly(LA). Control of polymer stereochemistry and molecular weight could possibly be achieved by altering the substituents in the guanidine and aryloxide ligands. Additional work in this area is currently under investigation.

Acknowledgment. We thank Dr. A. Khitrin (KSU) for assistance with the PGSE measurements, Dr. M. Gangoda (KSU) for assistance with the MALDI-TOF measurements, and J. A. Ocana (KSU) for assistance with elemental analysis. We thank Kent State University for financial support of this work.

Supporting Information Available: Thermal ellipsoid plots for **5** (Figure S1) and **9** (Figure S2). MALDI-TOF mass spectrum of PLA (Figure S3). This material is available free of charge via the Internet at http://pubs.acs.org. Crystallographic data (excluding structure factors) for the structures have been deposited with the Cambridge Crystallographic Data Centre as supplementary publication nos. CCDC 647796 for **1**, CCDC 647797 for **2**, CCDC 647798 for **3**, CCDC 647799 for **4**, CCDC 647800 for **5**, CCDC 647801 for **6**, CCDC 647802 for **7**, CCDC 647803 for **8**, and CCDC 647804 for **9**. Copies of the data can be obtained, free of charge, via http://pubs.acs.org or on application to CCDC, 12 Union Road, Cambridge CB2 1EZ, UK (fax, +44-(0)1223-336033; or e-mail, deposit@ccdc.cam.ac.uk).

OM700501G